we find that the $\frac{7}{2}^+$ ground state consists almost exclusively ($\sim$92%) of a $\frac{7}{2}^+$ single quasiparticle.

Again, with the wave functions from Ref. 32 Sorensen[34] calculated a value of 9.7 for the $E2$ enhancement for a $\frac{5}{2}^+$ to $\frac{7}{2}^+$ transition in ^{133}Cs. If the 81-keV state corresponds to the $\frac{5}{2}^+$ state of Ref. 32, then the experimental $E2$ enhancement of 26 for the 81-keV transition suggests that this state is more phonon-mixed than predicted by Kisslinger and Sorensen.[32] Furthermore, the even greater $E2$ enhancement for the 161-keV transition suggests that $\frac{5}{2}^+$ state at 161 keV is even more collective than the 81-keV state. Finally, similar qualitative arguments can be made from the $M1$ retardation factors about the nature of these $\frac{5}{2}^+$ states in ^{133}Cs.

Recently, Kisslinger and Kumar[35] have extended the pairing-plus-quadrupole model allowing for independent quasiparticle and collective motion with anharmonicity in the vibrational motion of the core included. It may be interesting to compare the present results with the predictions of that theory when the detailed results in this region of ^{133}Cs become available.

[35] L. S. Kisslinger and K. Kumar, Phys. Rev. Letters 19, 1239 (1965).

PHYSICAL REVIEW C VOLUME 1, NUMBER 1 JANUARY 1970

^{208}Pb(t, α)^{207}Tl and ^{207}Pb(t, α)^{206}Tl Reactions at 20 MeV*

P. D. Barnes,† E. R. Flynn, G. J. Igo, and D. D. Armstrong
Los Alamos Scientific Laboratory, University of California, Los Alamos, New Mexico 87544

(Received 20 June 1969)

The proton pickup reaction (t, α) has been used to investigate states in ^{207}Tl and ^{206}Tl. The angular distributions resulting from populating five states in ^{207}Tl which are predominantly single-hole in character have been analyzed to obtain spectroscopic factors. In the ^{207}Pb(t, α)^{206}Tl spectrum, doublets corresponding to the interaction of proton holes in the four lowest-lying orbits with a $3p_{1/2}$ neutron hole are the strongest states observed. The $2d_j$ proton-hole strength is found in several levels of ^{206}Tl. The positions and intensities of the observed levels are in quantitative agreement with the nuclear-structure calculations of Kuo.

I. INTRODUCTION

THE positions and relative spectroscopic factors of single-particle states in the one-particle and one-hole nuclei surrounding ^{208}Pb have been determined in recent research by a number of laboratories.[1–13] The results are summarized in Fig. 1, which shows the positions, spins, and parities of states in ^{209}Pb, ^{209}Bi, ^{207}Pb, and ^{207}Tl with large components of the shell-model single-particle states. With the exception of the cross-hatched and dashed levels, the relative spectroscopic factors are within $\pm$20% of the predictions of the shell model with no mixing. The cross-hatched levels, which have significantly lower spectroscopic factors, may also be understood within the framework of the shell model. The unperturbed positions of levels of the same spins and parities, but of a different character, lie in close proximity to the particular single-particle states, and the strength is fractionated between these levels. A few levels are dashed in Fig. 1 to indicate that relative spectroscopic strengths measured by different groups do not agree within $\pm$20%.

In order to test the validity of the shell model in the ^{208}Pb region further, we have studied states in ^{207}Tl and ^{206}Tl. The ^{208}Pb(t,α)^{207}Tl* reaction preferentially populates five levels in ^{207}Tl, shown in Fig. 1 as proton-hole excitations. The four lowest states in excitation energy are very strongly excited, while the excitation of the fifth state is considerably weaker.

According to the shell model, levels populated by the proton-pickup reaction on a ^{207}Pb target should be of a very simple character. The ground state of ^{207}Pb is almost a pure $p_{1/2}$ neutron-hole configuration $(3p_{1/2})_\nu^{-1}$ in the ^{208}Pb core. Therefore, in the simplest approximation, the ^{206}Tl spectrum will consist simply of four

* Work performed under the auspices of the U.S. Atomic Energy Commission.
† Present address: Physics Dept., Carnegie-Mellon University, Pittsburgh, Pa.
[1] R. Woods, P. D. Barnes, E. R. Flynn, and G. J. Igo, Phys. Rev. Letters 19, 453 (1967).
[2] J. S. Lilley and N. Stein, Phys. Rev. Letters 19, 709 (1967).
[3] N. Stein, R. H. Siemssen, and B. Zeidman, Bull. Am. Phys. Soc. 12, 1066 (1967).
[4] B. H. Wildenthal, B. M. Preedom, E. Newman, and M. R. Cates, Phys. Rev. Letters 19, 960 (1967).
[5] C. Ellegaard and P. Vedelsby, Phys. Letters 26B, 155 (1968).
[6] J. Bardwick and R. Tickle, Phys. Rev. 171, 1305 (1968).
[7] N. Auerbach and N. Stein (to be published).
[8] S. Hinds, R. Middleton, J. H. Bjerregaard, O. Hansen, and O. Nathan, Nucl. Phys. 83, 17 (1966).
[9] W. C. Parkinson, D. L. Hendrie, H. H. Duhm, J. Mahoney, J. Saudinos, and G. R. Satchler, Phys. Rev. 178, 1976 (1969).
[10] S. A. A. Zaidi and S. Darmodj, Phys. Rev. Letters 19, 1446 (1967); C. Ellegaard, J. Kantele and P. Vedelsby, Nucl. Phys. A129, 113 (1969).
[11] P. Mukherjee and B. L. Cohen, Phys. Rev. 127, 1284 (1962); C. Glashausser and M. E. Rickey, *ibid.* 154, 1033 (1967); G. Muehllehner, A. S. Poltorak, W. C. Parkinson, and R. H. Bassel, *ibid.* 159, 1039 (1967); W. P. Alford and D. G. Burke, private communication; K. Yagi, T. Ishimatsu, Y. Ishizaki, and Y. Saji, Nucl. Phys. A121, 161 (1968).
[12] G. J. Igo, P. D. Barnes, E. R. Flynn, and D. D. Armstrong, Phys. Rev. 177, 1831 (1969).
[13] F. P. Brady, N. F. Peek, and R. A. Warner, University of California, Davis, Report No. CNL-UCD23 (unpublished).

strong doublets. Each of the four low-lying, strongly excited proton-hole states observed in the ^{208}Pb$(t, \alpha)^{207}$Tl reaction would be split due to the $3p_{1/2}$ neutron-hole–proton-hole interaction. The doublet splitting extracted from the data can be used to determine the strength of the $3p_{1/2}$ neutron-hole–proton-hole interaction near $A=200$.

The mechanism for recognizing the four strong doublets in ^{206}Tl utilizes the observed shapes of the angular distributions for exciting the proton-hole states in the ^{208}Pb$(t,\alpha)^{207}$Tl reaction. Furthermore, the combined strength of the doublet members will be almost as large as the strength observed for each proton-hole excitation in the ^{208}Pb$(t, \alpha)^{207}$Tl reaction. The spectrum will be more complicated because of the presence of other neutron-hole–proton-hole (ν^{-1}, π^{-1}) states in ^{206}Tl in which ν is not a $3p_{1/2}$ neutron hole. Since states of the same spin and parity among the latter group can mix with the former, a relatively large number of less strongly excited transitions to states which have a large component with a neutron hole other than $3p_{1/2}$ will be observed. The existence of other hole-hole states in ^{206}Tl are already known from the ^{205}Tl$(d,p)^{206}$Tl reaction[14] and from the ^{205}Tl$(n, \alpha)^{206}$Tl reaction.[15] Indeed, a recent study of the ^{208}Pb$(d, \alpha)^{206}$Tl reaction[16] displays a multitude of such states. The same interaction which produces the mixing will also perturb the spacings of the doublets. Therefore, to determine the $3p_{1/2}$ neutron-hole–proton-hole interaction for the splittings of the four strong doublets, the effect of mixing on the doublet splitting will have to be accounted for.

The ^{208}Pb$(t,\alpha)^{207}$Tl reaction has been previously studied[8] at 12.0 and 13.5 MeV, and the results of that work can be summarized as follows: Four strongly excited proton-hole states plus the weakly excited $1g_{7/2}$ proton-hole state were observed and the relative spectroscopic strengths of the five states were reported. The results of the present work at 20 MeV substantiate the conclusions reached in Ref. 8. Because the effect of the Coulomb barrier is less important at 20 MeV, two qualitative differences appear. First, a substantial number of weakly excited states appear in the spectrum at higher excitations, and second, the angular distributions tend to contain stronger diffraction-like structure.

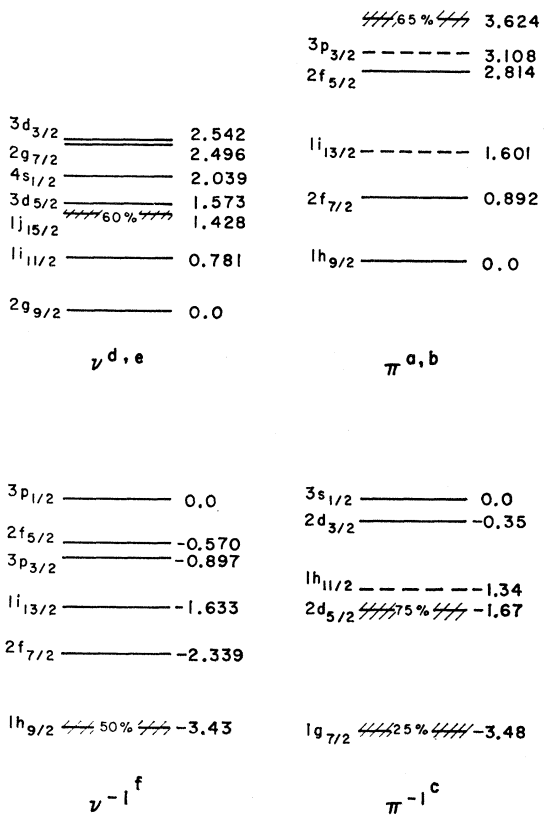

FIG. 1. Single-particle states in ^{208}Pb±one-nucleon nuclei. Cross-hatched levels have small spectroscopic strength relative to other levels. The percentages shown on the cross-hatched levels are relative strengths. Levels for which there is experimental ambiguity in the spectroscopic strength are dashed. (a) References 1–7. (b) The relative spectroscopic strengths of the 1.601 and 3.108-MeV levels obtained in Ref. 4 are 56 and 67% of their relative shell-model values; Refs. 2, 3, and 5 report relative spectroscopic factors near 100% for these levels. (c) References 8 and 9, and this paper. (d) References 10–12. (e) The values obtained in the work of Muehllehner *et al.*, (see Ref. 9) for the spectroscopic strengths of the $9/2^-$ and $15/2^-$ levels are lower and higher, respectively, than the values obtained in Ref. 12. The (t, d) reaction was studied in the latter reference. Because both tritons and deuterons are strongly absorbed, ambiguities associated with radial cutoff and optical potentials are absent. In the study of the (d, p) reaction (Ref. 9), well-known ambiguities associated with a weakly absorbed particle are observed and undoubtedly are the source of the discrepancies noted above. The (p, p') and (d, p) measurements of Ref. 8 corroborate the values obtained in the (t, d) reaction. See Refs. 9, 11, and 13.

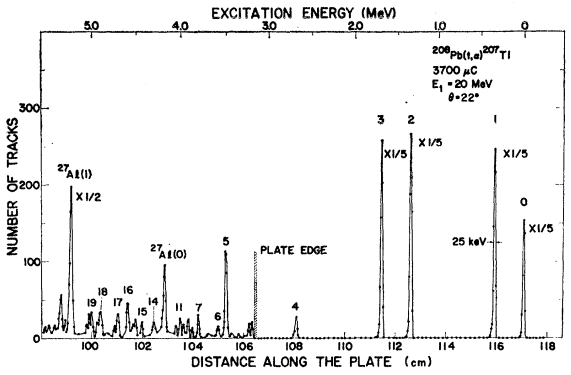

FIG. 2. Spectrograph data obtained in the ^{208}Pb$(t, \alpha)^{207}$Tl reaction. The number of tracks is plotted versus the distance along the focal plane (lower scale) and against the energy (upper scale). The numbered peaks are identified as states in ^{207}Tl.

[14] J. R. Erskine, Phys. Rev. **138**, B851 (1965).
[15] C. C. Weitkamp. J. A. Harvey, G. G. Slaughter, and E. C. Campbell, Bull. Am. Phys. Soc. **12**, 922 (1967), and private communication from C. C. Weitkamp.
[16] M. Lewis and W. W. Daehnick, Phys. Rev. Letters **22**, 77 (1969).

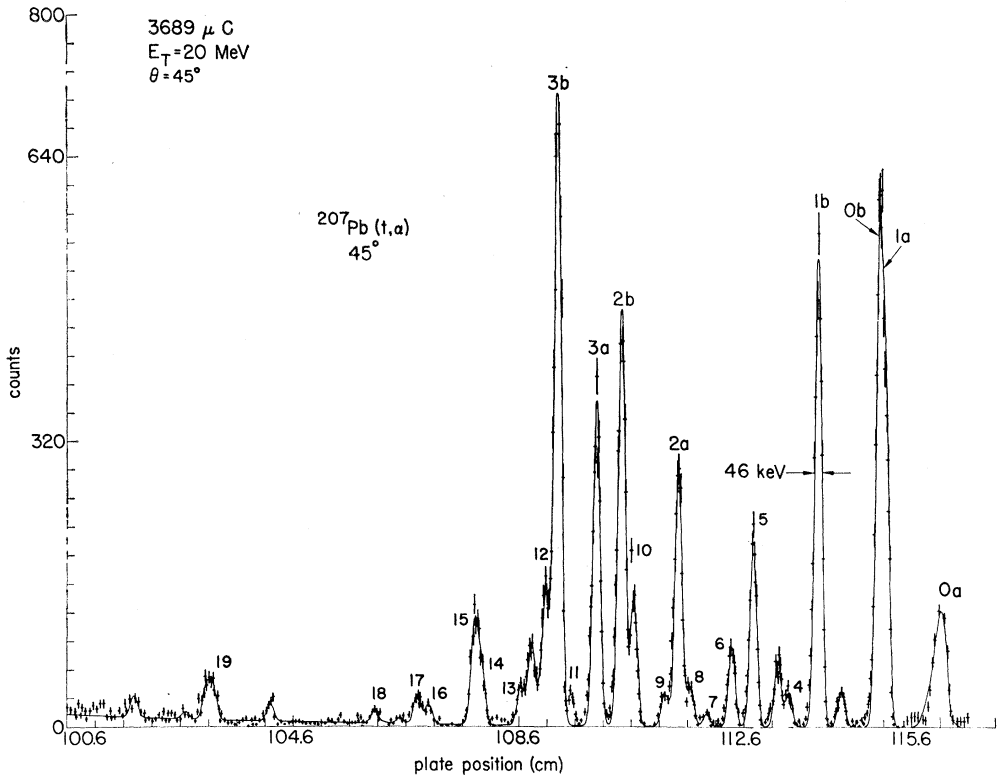

FIG. 3. Spectrograph data obtained in the ^{207}Pb(t, α) ^{206}Tl reaction. The seven strongest peaks in the spectrum are associated with four doublets 0a-b, 1a-b, 2a-b, and 3a-b which are discussed in the text. The resolution is 46 keV.

II. EXPERIMENTAL TECHNIQUE

The measurements were carried out at the Los Alamos tandem Van de Graaff facility. Both an Elbek-type magnetic spectrograph and a $\Delta E/\Delta X$-E counter telescope were used. These measurement techniques have been described in detail elsewhere.[12] In addition to the (t, α) reaction, the (t, p) and (t, d) reactions were studied simultaneously. Consequently, the target angles used were not optimum for maximum α-particle resolution. The absolute cross-section scale is based on that described in Ref. 12 for the ^{208}Pb target and on a similar measurement for the ^{207}Pb target.

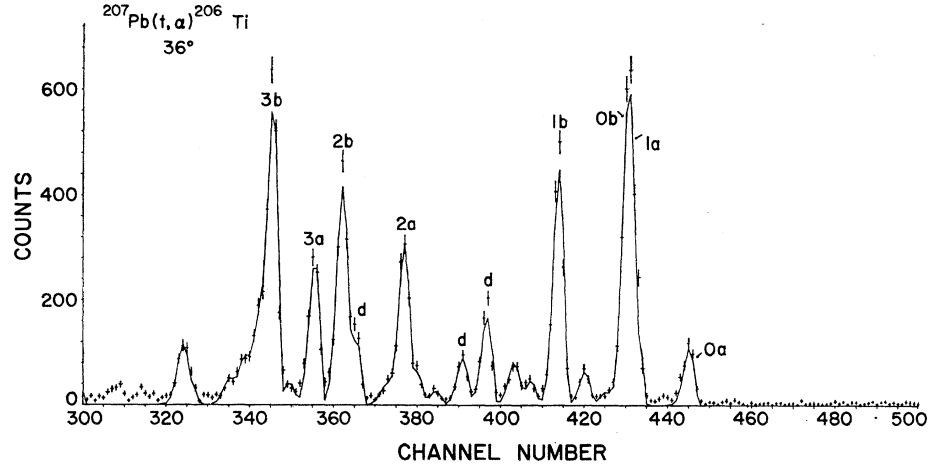

FIG. 4. Counter telescope data obtained in the ^{207}Pb$(t, \alpha)^{206}$Tl reaction. The seven strongest peaks in the spectrum are associated with four doublets 0a-b, 1a-b, 2a-b, and 3a-b, which are discussed in the text. The resolution is 50 keV.

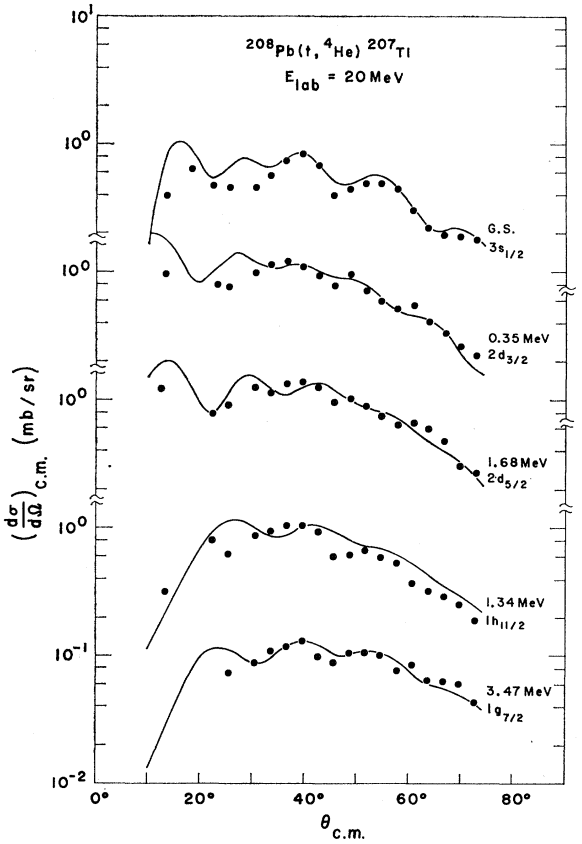

FIG. 5. Differential cross section for the proton pickup reaction on ^{208}Pb. Solid curves are DW fits.

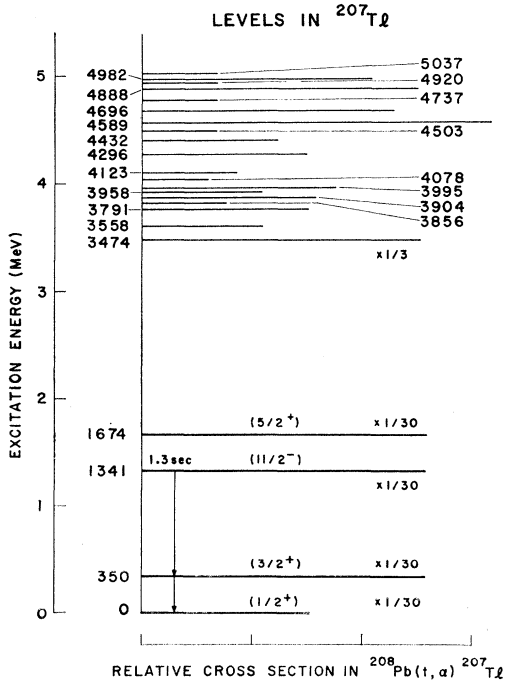

FIG. 6. Levels in ^{207}Tl observed in the ^{208}Pb$(t, \alpha)^{207}$Tl reaction.

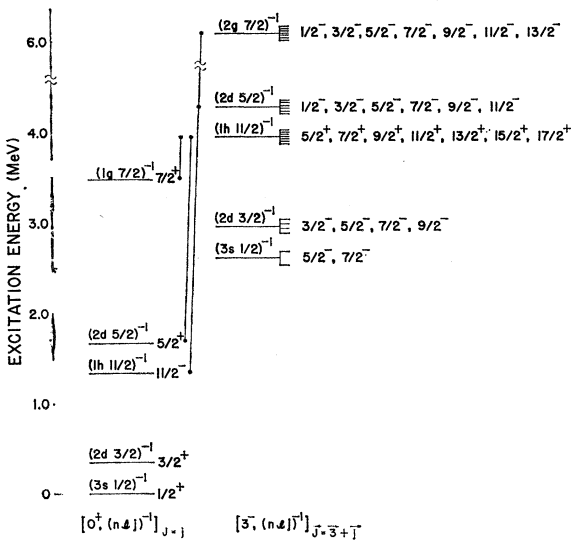

FIG. 7. Single-hole states in ^{207}Tl and core excitation multiplets. The $g_{7/2}^{-1}$ proton configuration is expected to be fragmented because of the proximity of members of the core-excited multiplets with the same spin and parity.

^{208}Pb$(t, \alpha)^{207}$Tl

A ^{208}Pb target 200 μg/cm^2 thick was exposed to the 20-MeV triton beam. The reaction products were analyzed in the angular range 30°–72° with the counter telescope, and in the 10°–30° range with the magnetic spectrograph (see Fig. 2). The resolutions for the two types of measurements were 43 and 25 keV, respectively.

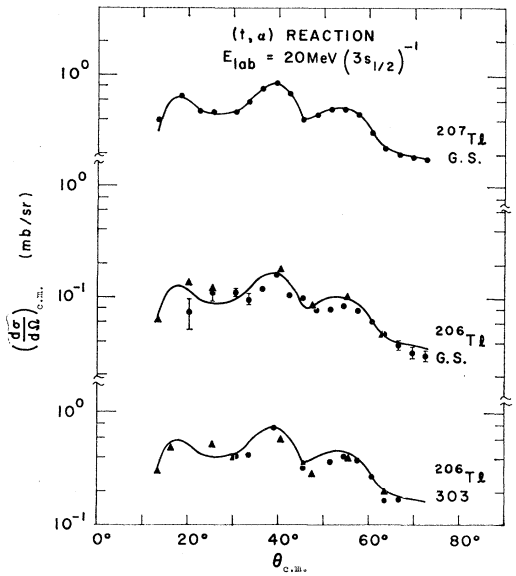

FIG. 8. Comparison of the angular distributions of the strong states populated by $l=0$ in the proton pickup reaction in ^{208}Pb and ^{207}Pb at low excitation. Spectrograph data indicated by a triangle; counter data, by a filled-in circle. Errors are smaller than the symbol's size unless an error flag is shown. Solid line is a smooth curve drawn through the ^{207}Tl data and used as a template for the ^{206}Tl data.

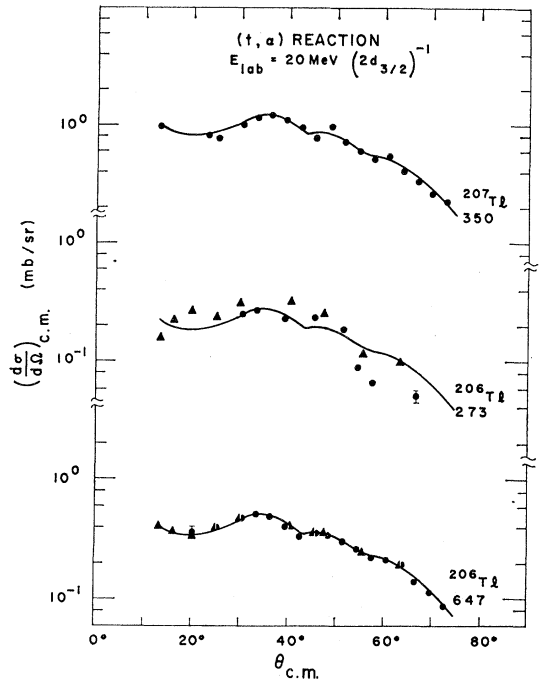

FIG. 9. Comparison of the strong states populated by $l=2$ in the proton pickup reaction on ^{208}Pb and ^{207}Pb at low excitation. Spectrograph data indicated by a triangle; the counter data by a filled-in circle. Errors are smaller than the symbol's size unless an error flag is shown.

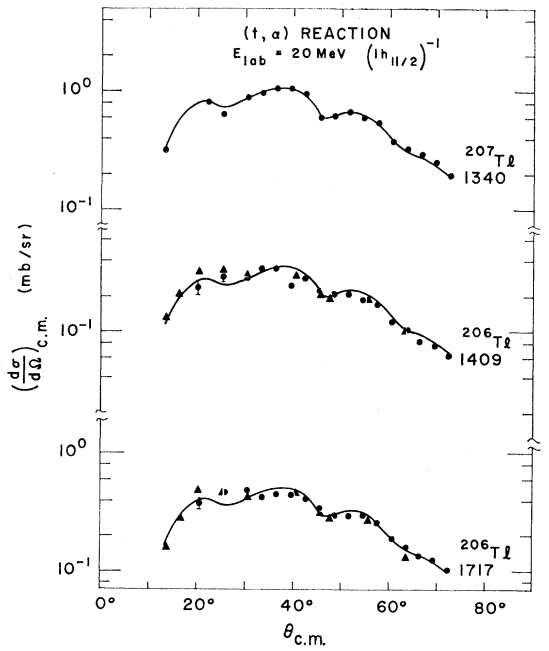

FIG. 10. Comparison of the strong states populated by $l=5$ in the proton pickup reaction in ^{208}Pb and ^{207}Pb. Spectrograph data indicated by a triangle; counter data, by a filled-in circle. Errors are smaller than the symbol's size unless an error flag is shown.

^{207}Pb(t, α)^{206}Tl

A ^{207}Pb target 200 μg/cm^2 thick was exposed to the 20-MeV triton beam. The reaction products were analyzed in the angular range 20°–72° with the counter telescope and in the 13°–63° (10 angles) range with the magnetic spectrograph. The resolution for the two types of measurements was about 45 keV. The spectrograph data were scanned in narrow bins (7 keV) to optimize the number of tracks per swath for scanning purposes (see Fig. 3). The counter telescope data were collected in wide bins (17 keV) (see Fig. 4). Although the resolution was about the same, the spectrograph data were most readily reduced to a spectrum of peaks because of the smaller bin size.

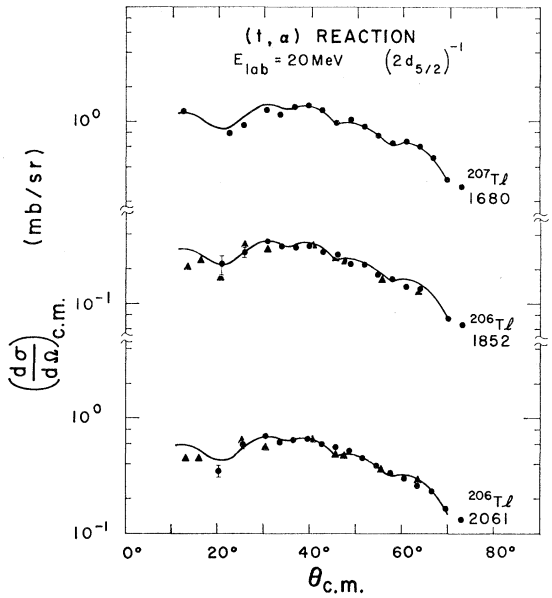

FIG. 11. Comparison of the strong states populated by $l=2$ in the proton pickup reaction in ^{208}Pb and ^{207}Pb at high excitation. Spectrograph data indicated by a triangle; counter data, by a filled-in circle. Errors are smaller than the symbol's size unless an error flag is shown.

Spectrum Analysis

Spectrograph data. The peak areas in the spectrograph data were obtained on a CDC 6600 computer using a peak fitting program developed at Los Alamos by Rickey. A well-resolved singlet in the spectrum is fit with a 6-parameter skewed Gaussian distribution with an exponential tail. Since the peak shape is principally determined by target-thickness effects in this experiment, the entire spectrum is unfolded with this peak shape fixed but allowing the following variables: (1) the number of peaks in the spectrum, (2) the position and height of each peak, and (3) the two-parameter background. The background is characterized

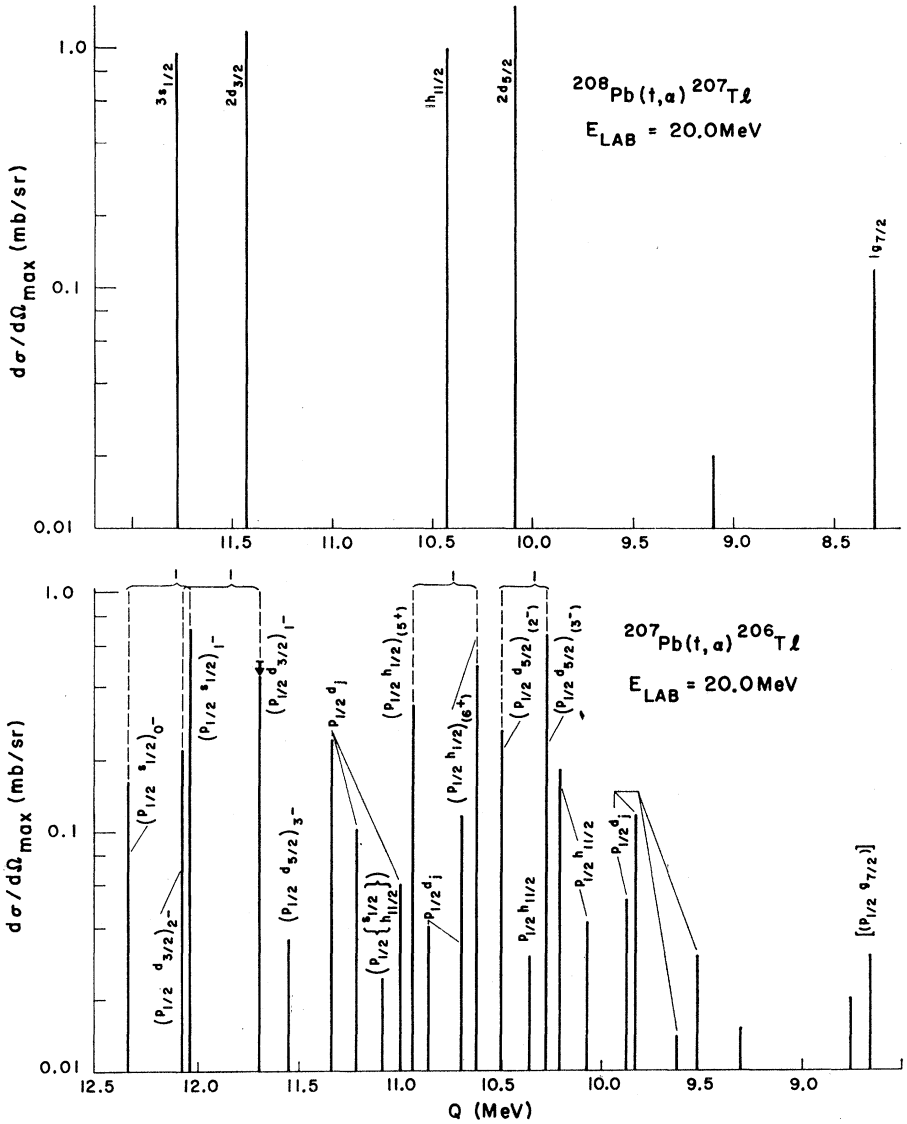

FIG. 12. Proton pickup line spectra obtained from ^{207}Pb and ^{208}Pb targets. Maximum differential cross section is plotted against the Q value. The abscissa has been shifted to align the position of the $(3s_{1/2}^{-1})_\pi$ state in ^{207}Tl with the centroid of the $(3p_{1/2}^{-1})_\nu(3s_{1/2}^{-1})_\pi$ doublet in ^{206}Tl. The peaks are identified by $(l_j l'_{j'})_J$, where l and j are quantum numbers for the neutron hole, and l' and j' are quantum numbers for the proton hole. The total spin-parity J_π is also given.

by a finite, constant value up to some specified point in the spectrum, followed by an exponential increase characterized by two variables, the initial value and the slope.

Counter telescope data. For the reason discussed above, the spectrograph data were easier to analyze than the counter telescope data. Therefore, the analysis using the peak-fitting program was altered from that described in the section on Spectrograph Data. As a starting condition, the total number of peaks and their approximate positions in the spectrum were fixed equal to the number and relative positions obtained from the spectrograph data.

III. RESULTS AND DISCUSSION

^{207}Tl

Five strongly excited states appear in the spectrum (see Fig. 2). These have been reported previously and tentative proton-hole configurations assigned as shown in Table I. Figure 5 shows the angular distributions which have been measured in this experiment. The solid curves represent distorted-wave Born-analysis (DWBA) calculations $\sigma_{DW}(\theta)$ [17] made with the computer code

[17] R. H. Bassel, R. M. Drisko, and G. R. Satchler, Oak Ridge National Laboratory Report No. ORNL-3240, 1962 (unpublished).

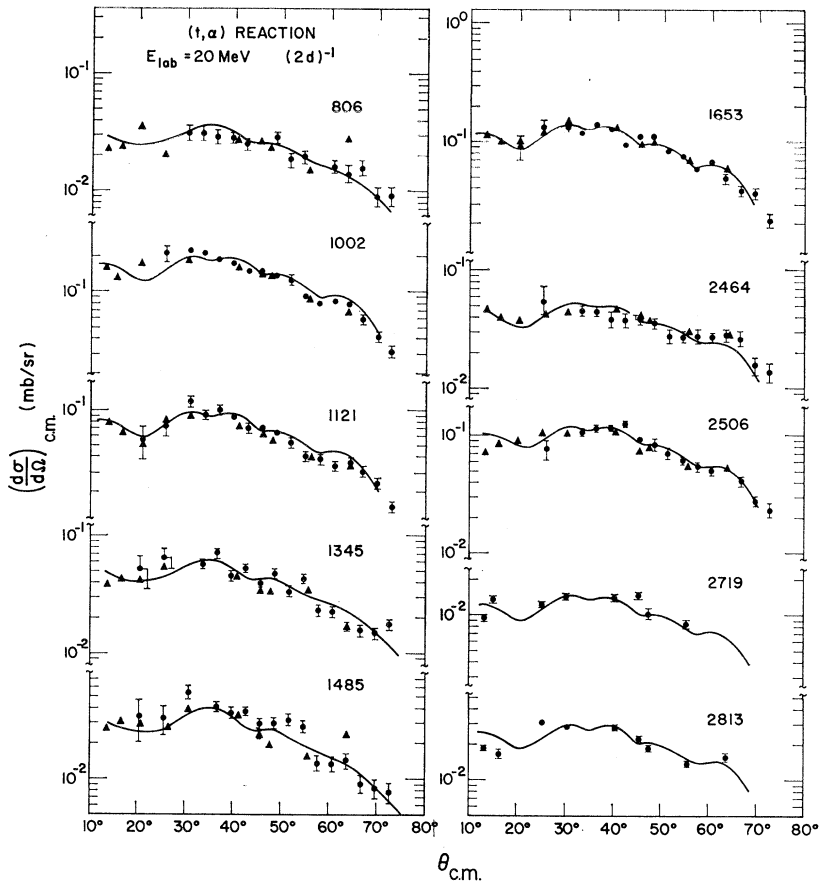

FIG. 13. Differential cross section for levels populated by $l=2$ transfers in the ^{207}Pb$(t, \alpha)^{206}$Tl reaction (see also Fig. 9). The level at 806 MeV is known to have spin-parity 3^- and, therefore, the state contains a $(3p_{1/2}^{-1})_\nu(2d_{5/2}^{-1})_\pi$ component.

JULIE written by Drisko. The experimental cross sections $d\sigma/d\Omega_{\text{exp}}$ are related to $\sigma_{\text{DW}}(\theta)$ by the following equation:

$$d\sigma/d\Omega_{\text{exp}}=NS_{lj}\sigma_{\text{DW}}(\theta).$$

The shell-model prediction for S_{lj} is $2j+1$. The value of the overlap integral between the proton-triton and α-particle wave functions determines N. Since the value of this integral has not been calculated, N is treated as a parameter to be determined which would be the same for all levels of ^{207}Tl analyzed in this experiment.

The detailed structure in the angular distributions is not reproduced in the calculation when triton parameters with depths up to 150 MeV which fit elastic-scattering data are used. These parameters had previously been used successfully in analyzing the ^{208}Pb$(t, d)^{209}$Pb data of Ref. 12. Table II lists the input parameters as well as the results of the (t, α) analysis. The optical-model parameters for α particles were taken from the work of Ref. 18.

The best fit to the $3s_{1/2}^{-1}$ (g.s.) proton-hole transition was obtained with a cutoff of 7.6 F. This value was adopted for the remainder of the analysis. The factor N was adjusted so that the spectroscopic factor for the $s_{1/2}^{-1}$, $d_{3/2}^{-1}$, and $h_{11/2}^{-1}$ states were optimized to agree with the shell-model values of the spectroscopic factors S_{lj} of the three states (see Table II). The $d_{5/2}^{-1}$ and $g_{7/2}^{-1}$ spectroscopic factors were then found to be 60 and 40% of their expected strength, respectively. A similar conclusion was reached from analysis of the 12.0- and 13.5-MeV data.[8] The normalization constant N is 54, compared with a value of 89 obtained in the Zr region with 20-MeV tritons.[19]

In addition to the five most intense levels discussed above, and previously reported,[8] new levels have been assigned up to 5-MeV excitation. Figure 6 and Table I show the level spectrum obtained in the ^{208}Pb$(t, \alpha)^{207}$Tl reaction, and the tentative spin assignments for the five most intense levels.[8] No attempt has been made to identify the l transfer for the higher states, primarily because the bulk of the angular distribution data was obtained with the counter telescope for which neither the resolution (43 keV) nor the statistics were sufficient to delineate clearly the angular distributions. The γ-ray transitions[20] between the 1341-keV isomeric level, the 350-keV level, and the ground state (see Fig. 6)

[18] L. McFadden and G. R. Satchler, Nucl. Phys. **84**, 177 (1966).

[19] D. D. Armstrong, A. G. Blair, and E. R. Flynn (unpublished).

[20] D. Eccleshall and M. J. L. Yates, Phys. Letters **19**, 301 (1965).

substantiate the assigned shell-model orbits for these states. This can be seen by considering the following evidence. First, the isomerism for the 1341-keV state is to be associated with high spin $(\frac{11}{2}^-)$; second, the measured lifetime of 1.3 sec for the 1341→350-keV transition while longer than the single-particle estimate for an $M4$ transition, gives a retardation factor consistent with other known $M4$ transitions[21]; third, if the 350-keV state were the $3s_{1/2}^{-1}$ state, and the ground state were the $2d_{3/2}^{-1}$ state, the single-particle estimate for an $M5$ transition to the 350-keV state would yield a lifetime 400 times larger than that observed, and also an $M4$ cross-over transition to the ground state would predominate. The latter transition is not observed.

As discussed above, the single-hole strength of the $(1g_{7/2})^{-1}$ orbit is 40%, and that of the $(2d_{5/2})^{-1}$ is 60%. Figure 7 illustrates the five most intense states observed which are mainly single-particle configurations $[0^+, (nlj)^{-1}]_{J=j}$ and the unperturbed positions of the core-hole excitation $[3^-, (nlj)^{-1}]_{J=3+j}$. Appreciable mixing between the $1g_{7/2}^{-1}$ level and the core excited state of the same spin-parity in the $[3^-, (1h_{11/2})^{-1}]$ multiplet is expected because of their proximity.

TABLE I. Levels in ^{207}Tl observed in the ^{208}Pb(t, α) ^{207}Pb reaction. The uncertainties in the relative positions of the energy levels is ±6 keV. Tentative assignment of the spin, parity, and principal quantum numbers nlj_π as well as the orbital angular momentum transfer l_π are listed.

Level no.	E_x (keV) ±6 (keV	l_π	nlj^π
0	g.s.	0	$3s_{1/2}^+$
1	350	2	$2d_{3/2}^+$
2	1341	5	$1h_{11/2}^-$
3	1674	2	$2d_{5/2}^+$
4	3474	(4)	$(1g_{7/2}^+)$
5	3558		
6	3791		
7	3856		
8	3904		
9	3958		
10	3995		
11	4078		
12	4123		
13	4296		
14	4432		
15	4503		
16	4589		
17	4696		
18	4737		
19	4888		
20	4920		
21	4982		
22	5037		

[21] M. Goldhaber, A. W. Sunyar, *Alpha-, Beta-, and Gamma-Ray Spectroscopy*, edited by Kai Siegbahn (North-Holland Publishing Company, Amsterdam, 1955), Vol. II, p. 946.

TABLE II. (a) The optical-model parameters used for the triton and α-particle wave functions. The depths V and W, radii r_R and r_I, diffuseness a_R and a_I, and Coulomb radius r_C of the real and imaginary potentials are listed. (b) The excitation E_x and the spectroscopic factor S_{ij} for each proton-hole state using a normalization factor, $N=54$.

(a)

Particle	V (MeV)	W (MeV)	r_R (F)	r_I (F)	a_R (F)	a_I (F)	r_C (F)
t	150.3	13.9	1.24	1.42	0.707	0.816	1.25
α	177.3	15.6	1.34	1.34	0.569	0.569	1.34

(b)

Orbit	E_x (MeV)	S_{ij}
$s_{1/2}$	0	1.9
$d_{3/2}$	0.350	4.6
$h_{11/2}$	1.341	10.7
$d_{5/2}$	1.677	3.7
$g_{7/2}$	3.474	3.2

Mixing of particle-core configurations into the $\frac{5}{2}^+$ hole state is also possible. Higher-lying multiplets based on other particle-hole excitations of the ^{208}Pb core can possibly mix but to a lesser extent because they are further away.

^{206}Tl

Figures 3 and 4 show spectrograph and counter-telescope spectra obtained in the ^{207}Pb$(t,\alpha)^{206}$Tl reaction. In general, the most intense peaks are members of the doublets associated with the four lowest-lying single proton-hole states populated in the ^{208}Pb$(t,\alpha)^{207}$Tl spectrum (see Fig. 2). The states 0a-b are identified as a doublet which is primarily $(2p_{1/2})_\nu^{-1}$ coupled to the most weakly bound proton-hole configuration $(3s_{1/2})_\pi^{-1}$. The identification from the angular distribution data is shown in Fig. 8. The observed angular distribution for the transition to the $(3s_{1/2})_\pi^{-1}$ level in ^{207}Tl (solid line and experimental points at the top) is used as a pattern to identify the members of the corresponding doublet in ^{206}Tl. Similarly, the states 1a-b, 2a-b, and 3a-b are identified as the doublets associated with the transitions to the $(2d_{3/2})_\pi^{-1}$, $(1h_{11/2})_\pi^{-1}$, and $(2d_{5/2})_\pi^{-1}$ configurations in Figs. 9–11. Figure 12 and Table III summarize the information which has been gained about the states which are primarily a $(3p_{1/2}^{-1})_\nu(nlj^{-1})_\pi$ configuration in ^{206}Tl. The first and second columns of Table III list the excitation energies and the quantum numbers of the proton-hole configurations in the doublets identified using the ^{207}Pb$(t, \alpha)^{206}$Tl reaction. The third column lists their spins and parities. The four tentative values are assigned on the basis of intensity (see column 4 of Table III). The intensity of the $2d_{3/2}^{-1}$ doublet member at 273 keV (in parentheses in Table III) is difficult to

TABLE III. The $[(3p_{1/2})_\nu^{-1}(nlj)_\pi^{-1}]_{J=j\pm1/2}$ states in ^{206}Tl. The quantity $\sigma_{\max}{}^J(^{206}\mathrm{Tl})$ is the maximum value of the observed differential cross section for the state with tentative spin assignment J; $\sigma_{\mathrm{STAT}}{}^J$ and σ_{Kuo} are predicted cross sections defined in the text. The centroids $E_x(^{206}\mathrm{Tl})$ are shifted by 239 keV in order to compare with the spacings of the ^{207}Tl spectrum, $E_x(^{207}\mathrm{Tl})$. The experimental ratio R is defined in Sec. III.

E_x (keV)	nlj	J^π	$\sigma_{\max}{}^J(^{206}\mathrm{Tl})$ (mb)	$\sigma_{\mathrm{STAT}}{}^J(j)$ (mb)	$\sigma_{\mathrm{Kuo}}{}^J$ (mb)	$E_x(^{206}\mathrm{Tl})$ -239 keV	$E_x(^{207}\mathrm{Tl})$ keV	R
0	$3s_{1/2}$	0^-	0.16	0.24	0.20	0	0	0.90
303	$3s_{1/2}$	1^-	0.60	0.71	0.66			
273	$2d_{3/2}$	2^-	(0.30)	0.76	0.43	267	350	$\leq$0.68
647	$2d_{3/2}$	1^-	$\leq$0.52	0.46	0.41			
1409	$1h_{11/2}$	(5^+)	0.35	0.46	0.29	1361	1340	0.83
1717	$1h_{11/2}$	(6^+)	0.53	0.54	0.47			
1852	$2d_{5/2}$	(2^-)	0.26	0.63	0.34	1762	1670	0.66
2061	$2d_{5/2}$	(3^-)	0.66	0.87	0.74			

obtain because it is not completely resolved from the stronger 303-keV state. The 647-keV peak is possibly a doublet[14,15] and, therefore, the measured strength is an upper limit. Besides the tentative spins assigned to four of the doublet members based on their relative intensities, some spin assignment already exist from the (d, p) [14] and (n, γ) [15] reaction results discussed in Sec. IV.

The fourth column lists the observed maximum cross sections for these states. The cross sections labeled σ_{STAT} in column 5 are the maximum cross sections expected for these doublets based on the cross sections observed for the corresponding orbits in ^{207}Tl and taking statistical factors into account, viz.,

$$\sigma_{\mathrm{STAT}}{}^J(j) = |(2J+1)/2(2j+1)|\,\sigma_{\max}{}^{nlj}(^{207}\mathrm{Tl}).$$

Comparison of columns 4 and 5 suggests that the ground state has only 65% of the expected single-particle $(s_{1/2}^{-1})_\pi$ strength, and that the strength of the $J^\pi=2^-$ states is more fragmented than that of the high-spin states. This result is consistent with the observation of so many levels excited below 3 MeV in ^{206}Tl as compared to the simple spectrum of ^{207}Tl. Column 6 lists the predicted cross sections for these states using the wave functions calculated by Kuo[22] and discussed in Sec. IV.

The centroids of the doublets $E_x(^{206}\mathrm{Tl})$ in ^{206}Tl and the positions of the corresponding proton-hole states in ^{207}Tl, $E_x(^{207}\mathrm{Tl})$, are compared in Fig. 12 and columns 7 and 8 of Table III. In Fig. 12 they are shown as short vertical lines above the brackets, and the Q-value scales have been adjusted to align the centroid of the $(3s_{1/2})_\pi^{-1}$ doublet with the $3s_{1/2}^{-1}$ proton-hole state in ^{207}Tl. The centroid spacings (Table III, column 7) are similar to the proton-hole spectrum (column 8). The last column in Table III compares the summed strength of the two members of the doublet (column 4) with the strength of the proton-hole configuration. In the absence of configuration mixing, one expects

$$R=[\sigma^{206}(j-\tfrac{1}{2})+\sigma^{206}(j+\tfrac{1}{2})]/\sigma^{207}(j)=1.$$

The doublets taken together are 70–90% as strong as the corresponding proton-hole state in ^{207}Tl.

It should be noted that the doublet splittings range between 209 and 374 keV and do not show a systematic dependence on spin. The spacing between the members of each doublet is undoubtedly influenced by the presence of nearby states of the same spin and parity (see Sec. IV).

States Containing a $(3p_{1/2}{}^{-1})(nlj^{-1})$ Configuration

Twenty-four states in the first 3.9-MeV excitation of ^{206}Tl have been identified in the spectrum of the ^{207}Pb$(t, \alpha)^{206}$Tl reaction (Fig. 3 and Table IV) within the limits of the α resolution. Table IV, columns 8–13, lists the level number, the energies, the assigned proton orbital angular momentum transfers, the maximum cross sections, the possible spin-parity values of the final state, and the probable orbit from which the proton was picked up. The portions of the levels listed in Table IV are identified by the level numbers in Fig. 3. These are compared in Table IV with the corresponding quantities obtained in the (d,p) and (n, γ) reactions as identified in Refs. 14 and 15. There is good agreement among the three reactions on the positions of low-lying energy levels which all three reactions populate. Because the target spin is $\frac{1}{2}$ in the (t, α) reaction, in principle the proton transfer could proceed via two different l_p values for the $J^\pi=3^-$ and 1^- states. The former involves (in addition to $d_{5/2}$ transfers) $l=4$ transitions, which are expected to be important only at high excitation and to have small cross section. None have been assigned. The latter involves both $s_{1/2}$ and $d_{3/2}$ transfers. If most of the $3s_{1/2}$ strength is in the ground and 303-keV states as Table III suggests, then this ambiguity will not confuse the interpretation of the observed cross sections.

[22] T. Kuo (private communication).

TABLE IV. Energy levels, configurations, and spin-parities observed in the (n, γ)[a] and (d, p)[b] reaction on ^{205}Tl and in the (t, α) reaction on ^{207}Pb. The maximum cross section $d\sigma$ for the (d, p) and (t, α) reaction are listed. The uncertainty in the relative position of the levels in the (t, α) reaction is ± 10 keV.

(n, γ)		(d, p)					Level	(t, α)				
E_x	J^π	E_x	l_p	$d\sigma$	J^π	$(nlj)_p$	No.	E_x	l_n	$d\sigma$	J^π	$(nlj)_n$
0	0⁻	0	1	0.42	0⁻	$p_{1/2}$	0[a]	0	0	0.16	0⁻	$3s_{1/2}$
266.1	2⁻	263	3	0.11	2⁻	$f_{5/2}$	1[a]	273	2	0.30	2⁻	$2d_{3/2}$
304.9	1⁻	305	1	1.30	1⁻	$p_{1/2}$	0[b]	303	0	0.60	1⁻	$3s_{1/2}$
635.3	2⁻	635	(1)	0.56	2⁻	$p_{3/2}$						
650.0	1⁻	650	(3)	0.24	1⁻[d]	$(f_{5/2})$	1[b]	647	2	0.52	1⁻	$2d_{3/2}$
801.6	3⁻	802		0.18	3⁻[c]	$f_{5/2}$	4	806	2	0.035	3⁻	$2d_{5/2}$
998.4		998		0.13			5	1002	2	0.24	1⁻, 2⁻, 3⁻	
1079.9												
1117.3		1117		0.13			6	1121	2	0.1	1⁻, 2⁻, 3⁻	
1204.8							7	(1257)	(0, 5)	0.024	0⁻, 1⁻, 5⁺, 6⁺	$3s_{1/2}$
1360.5		1335		0.06			8	1345	2	0.06	1⁻, 2⁻, 3⁻	
1453.0							2[a]	1409	5	0.35	5⁺, (6⁺)	$1h_{11/2}$
1489.8							9	1485	2	0.04	1⁻, 2⁻, 3⁻	
1631.3							10	1653	2	0.134	1⁻, 2⁻, 3⁻	
							2[b]	1717	5	0.53	6⁺, (5⁺)	$1h_{11/2}$
1842.1							3[a]	1852	2	0.26	2,⁻ (1⁻, 3⁻)	$(2d_{5/2})$
1992.5							11	1985	5	0.03	5⁺, 6⁺	$1h_{11/2}$
							3[b]	2061[d]	2	0.66	3⁻, (1⁻, 2⁻)	$(2d_{5/2})$
							12	2128[d]	5	0.18	5⁺, 6⁺	$1h_{11/2}$
							13	2264	5	0.04	5⁺, 6⁺	$1h_{11/2}$
							14	2464	2	0.05	1⁻, 2⁻, 3⁻	
							15	2506	2	0.115	1⁻, 2⁻, 3⁻	
		2581		1.1								
		2594		1.0								
							16	2717	2	0.014	1⁻, 2⁻, 3⁻	
							17	2813	2	0.03	1⁻, 2⁻, 3⁻	
		2828		0.43								
		2868		0.30								
		2896		0.18								
		3014		0.38				3022		0.015		
		3363		0.48								
		3424		0.24								
		3452		0.62								
		3538		0.24								
		3564		0.18								
		3638		0.92								
		3717		0.11								
		3784		0.51								
								3865	(4)	0.05	(3⁻, 4⁻)	$(1g_{7/2})$

[a] Reference 15.
[b] Reference 14.
[c] Spin assignments are not Erskine's but due to Harvey (n, γ), and are consistent with Erskine's data.
[d] Possibly a doublet, see Sec. III.

Some of the peaks observed in the ^{207}Pb(t, α)^{206}Tl reaction may be complex, and specific cases where this situation may exist are noted. Whenever possible, we use existing data[14,15] to determine spins and parities. As in the case of the four strong doublets, the l-transfer identification is made by comparison with the angular distributions obtained in the ^{208}Pb(t, α)^{207}Tl. In Figs. 13 and 14, the angular distributions of levels populated by $l=2$ and $l=5$ angular momentum transfers in the ^{207}Pb(t, α)^{206}Tl reaction are shown (the four strong doublets are not included). The lines through the experimental points are empirical fits to the $l=2$ and $l=5$ transfer data obtained in the ^{208}Pb(t, α)^{207}Tl reaction. In the (d, p) reaction,[14] six energy levels below 1-MeV excitation in ^{206}Tl are strongly excited. The states are formed primarily by coupling an $s_{1/2}$ proton hole with $p_{1/2}$, $f_{5/2}$, or $p_{3/2}$ neutron holes. However, it should be pointed out that the target nucleus in the (d, p) reaction, ^{205}Tl, is known to be 75% $s_{1/2}$ proton-hole configuration, with the remainder being $d_{3/2}$ and $d_{5/2}$ proton-holes coupled to the 2⁺ quadrupole vibration of ^{206}Pb.[20,21] Therefore, the weakly excited states in ^{206}Tl

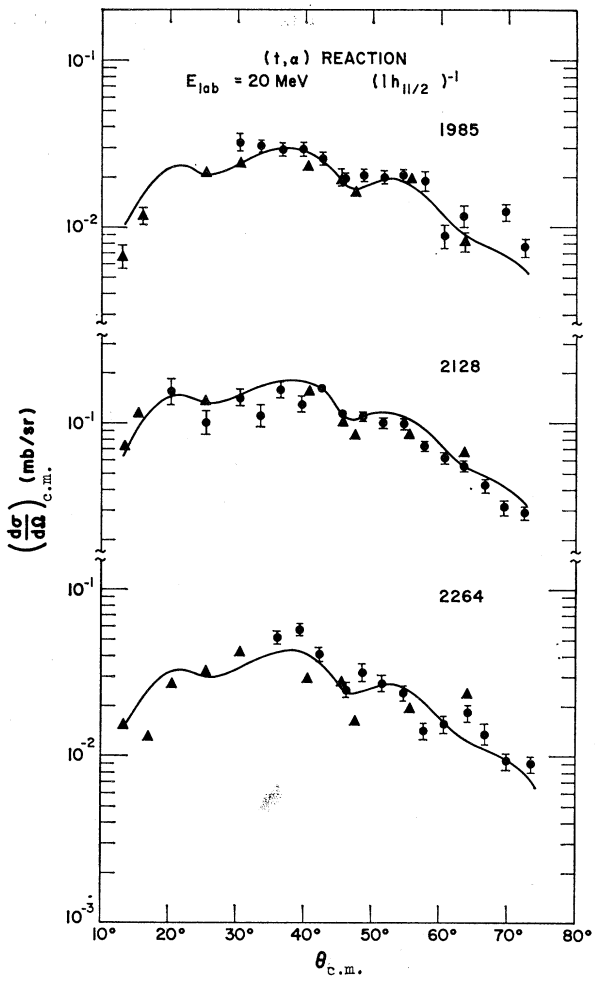

FIG. 14. Differential cross section for levels populated by $l=5$ transfers in the ^{207}Pb$(t, \alpha)^{206}$Tl reaction (see also Fig. 10).

populated by the (d, p) reaction may contain more complicated neutron-hole configurations. The ground state and the 305-keV level are populated by $l=1$ and $l=0$ transfers in the ^{205}Tl$(d, p)^{206}$Tl reaction[14] and in the ^{207}Pb$(t, \alpha)^{206}$Tl reaction, respectively. This completely specifies the major component of those levels, the $(p_{1/2}^{-1})_\nu(s_{1/2}^{-1})_\pi$ configuration. The 273-keV state is strongly populated by an $l=2$ transfer in the (t, α) reaction, and populated by an $l=3$ transfer in the (d, p) reaction. Two components of this state are, therefore, $(p_{1/2}^{-1})_\nu(d_{3/2}^{-1})_\pi$ and $(f_{5/2}^{-1})_\nu(s_{1/2}^{-1})_\pi$ to be consistent with a 2^- spin assignment.[14,15] Both of these can be formed in the (d, p) reaction.

In the (d, p) reaction, the strongly excited 635-keV level is not clearly resolved at all angles from the 650-keV level; therefore, the l value of the former is not completely determined. The 635-keV state is assigned in Ref. 14 as the 2^- member of the $(p_{3/2}^{-1})_\nu(s_{1/2}^{-1})_\pi$ doublet. The 650-keV state was tentatively assigned in Ref. 14 as a 3^- state. However, the (n, γ) experiment[15] suggests the 802-keV state rather than the 650-keV state is the 3^- member of the $(f_{5/2}^{-1})_\nu(2s_{1/2}^{-1})_\pi$ configuration, and that the 650-keV state has $J^\pi=1^-$. This assignment is still in agreement with the application of the sum rules to Erskine's (d, p) intensities according to the authors of Ref. 15. The (t, α) reaction strongly excites a level at 647 keV with $l=2$, as expected.

However, the intensity ratio measured in the (t, α) reaction is in disagreement with the assignment for the spins of the $(p_{1/2}^{-1})_\nu(d_{3/2}^{-1})_\pi$ doublet (273 and 647 keV) as determined in the (n, γ) measurement. The cross section for the 647-keV state is an upper limit, since the 635-keV state is unresolved. The intensity ratios of the $d_{5/2}^{-1}$ and $d_{3/2}^{-1}$ doublets are the least reliable for determining the spin-parities, since many of the weakly excited states in Fig. 3 contain a d_j^{-1} proton configuration and may, therefore, significantly distort the position, splitting, and intensities of these doublet members. This configuration mixing for the 273- and 647-keV levels is suggested by the fact that $l_\nu=3$ transfers are observed to these levels in the (d, p) reaction, although $l_\nu=1$ transfers would be expected. A level at 517 keV in Fig. 3 is due to ^{208}Pb contamination in the target.

The 3^- assignment to the 802-keV state means that this state has a small component of the $(p_{1/2}^{-1})_\nu(d_{5/2}^{-1})_\pi$ configuration because it is populated weakly in the (t, α) reaction with $l=2$ transfer. A level at 871 keV in Fig. 3 is due to ^{208}Pb contamination in the target.

States at 1002, 1121, and 1345 keV are identified by the $l=2$ transfer in the (t, α) reaction (see Fig. 13) to be of spin 1^-, 2^-, or 3^-. In the (d, p) experiment,[14] these three states are populated by $l=2$ transfers (see the 998-, 1117-, and 1335-keV states in Table IV). Consequently, they probably contain in addition a weak component with an $s_{1/2}^{-1}$ proton configuration. No states are populated in the (d, p) reaction between 1335 and 2581 keV—which is the expected result, since the wave function of ^{205}Tl [23,24] contains essentially only $p_{1/2}$, $p_{3/2}$, and $f_{5/2}$ neutron holes.

Returning to the discussion of the (t, α) results, there is some evidence for a weakly excited state at about 1670 keV which may lie in the shoulder between the 1653- and 1717-keV states (see Fig. 3). It is not listed in Table IV because it cannot be positively identified. The 1717- and 1852-keV states have been discussed previously. The 1340-keV $(1h_{11/2}^-)$ state in ^{207}Tl arising from the ^{208}Pb contaminant falls at the same position in the spectrum as the 1852-keV level with 25% of the strength of the former.

The 1985-keV level is populated by an $l=5$ angular momentum transfer. The 2061-keV peak may be an unresolved doublet, with the weaker member on the

[23] O. Nathan, in *Proceedings of the International Symposium on Nuclear Structure, Dubna, 1968* (unpublished).

[24] O. Nathan. G. Bruce, A. Bussierne, P. Kossanyi, J. M. Loiseaux, P. Roussel, J. Testoni, and L. Valentin, Nucl. Phys. A109, 481 (1968).

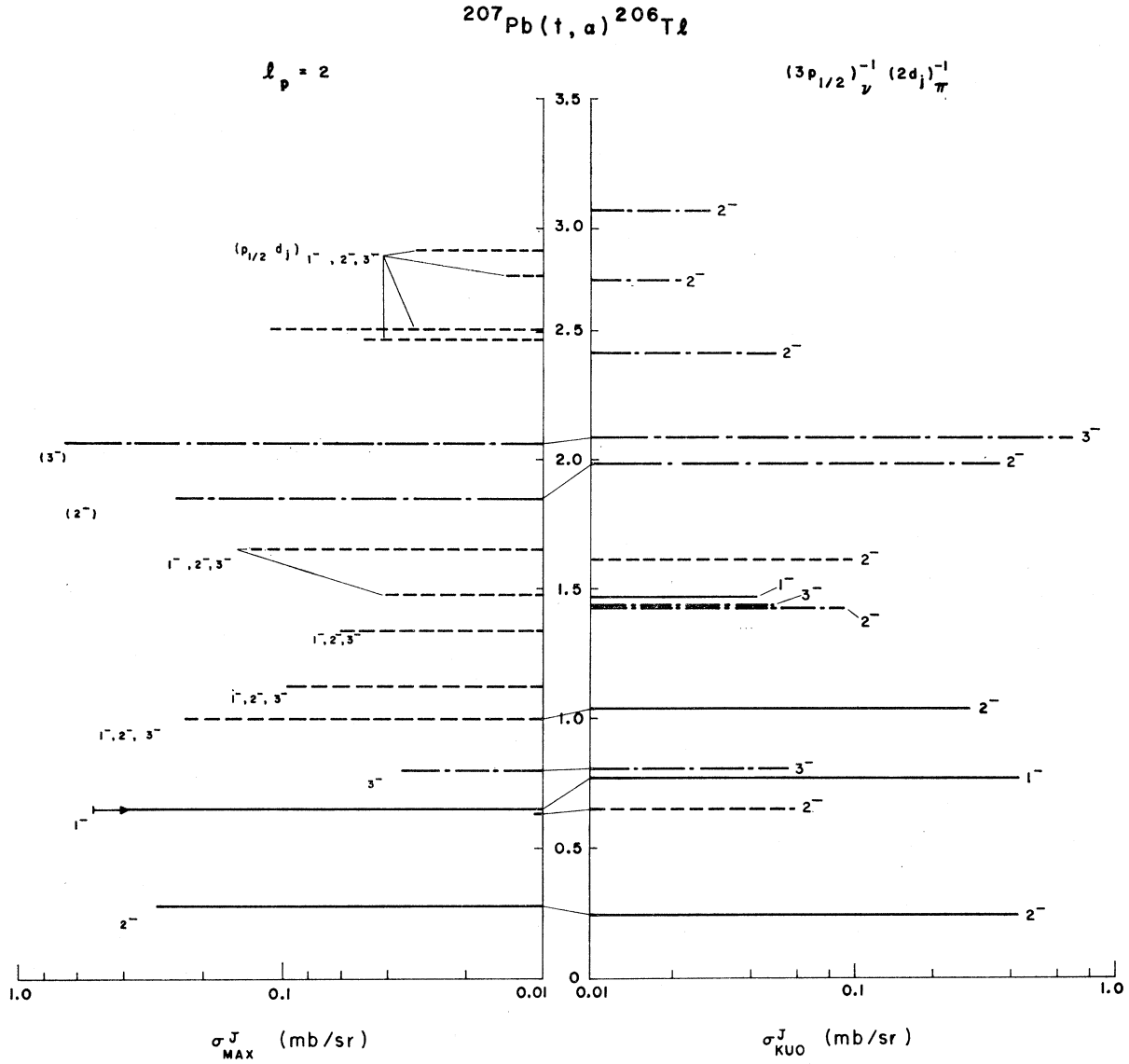

FIG. 15. Comparison of levels populated with $l=2$ transfer to the levels calculated by Kuo (Ref. 22) with a $(3p_{1/2}^{-1})_\nu(2d_{3/2}^{-1})_\pi$ and/or a $(3p_{1/2}^{-1})_\nu(2d_{5/2}^{-1})_\pi$ component. The levels represented by solid lines in the experimental spectrum are identified as having a $(3p_{1/2}^{-1})_\nu(2d_{3/2}^{-1})_\pi$ component; by dash-dot lines, a $(3p_{1/2}^{-1})_\nu(2d_{5/2}^{-1})_\pi$ component; and by dashed lines, either or both components. In the calculated spectrum, the levels represented by solid lines have a large component of $(3p_{1/2}^{-1})_\nu(2d_{3/2}^{-1})_\pi$; by dash-dot lines, a large component of $(3p_{1/2}^{-1})_\nu(2d_{5/2}^{-1})_\pi$; and by dashed lines, about equal amounts of each component. The thin lines between the theoretical spectrum and the experimental spectrum connect levels which probably correspond to one another.

higher excitation shoulder. The angular distribution for the peak displays an $l=2$ proton-transfer pattern (see Fig. 11) and is expected to be a $[(3p_{1/2}^{-1})_\nu(2d_{5/2}^{-1})_\pi]_{3^-}$ configuration.[14,15] The peak at 2128 keV may be complex, and because it is sandwiched between the large 2061-keV peak and the $(d_{5/2}^{-1})_\nu$ level from the ^{208}Pb(t, α)^{207}Tl contaminant reaction at 2204 keV in the spectrum (see Fig. 3), it is impossible to determine whether or not it is a single state. The angular distribution of the 2128-keV state is distinctly that of an $l=5$ proton transfer suggesting that it may be a singlet. The 2264-keV state is populated by an $l=5$ transfer reaction.

The broad peak containing the 2464- and 2506-keV states may also contain a third, weakly excited state at about 2530 keV. The 2506-keV state, however, is clearly populated by an $l=2$ transfer. Above 2580 keV, one-particle two-hole neutron configurations are excited in the (d, p) reaction,[14] and isobaric analogs of some of these are observed in the ^{205}Tl(p, p')^{205}Tl* reaction.[25]

[25] W. Hering (private communication).

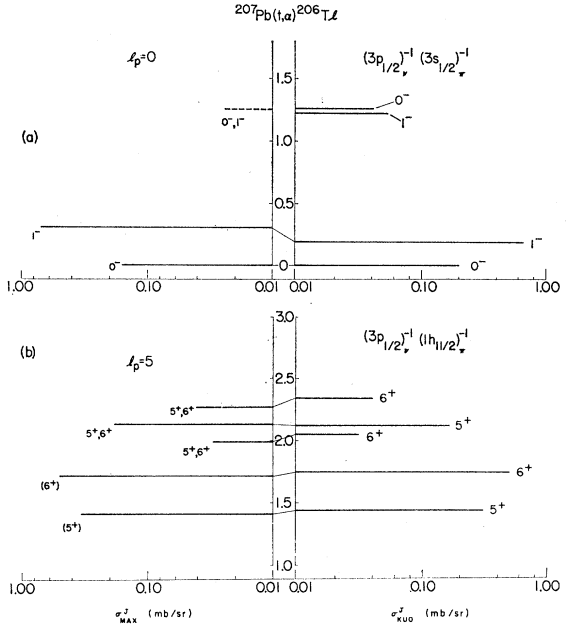

FIG. 16. (a) Comparison of levels populated by an $l_p=0$ transfer in the ^{207}Pb$(t, \alpha)^{206}$Tl reaction with the calculated cross section for levels with a $(3p_{1/2}^{-1})_\nu((3s_{1/2}^{-1})_\pi$ component. The $l_p=0$ assignment to the dashed level in the experimental spectrum is quite uncertain. (b) Comparison between levels populated by an $l_p=5$ transfer with the calculated cross section for levels with a $(3p_{1/2}^{-1})_\nu(1h_{11/2}^{-1})_\pi$ component.

Two more states at 2717 keV and 2813 keV are observed in the ^{207}Tl$(t, \alpha)^{206}$Tl reaction which are populated by $l=2$ angular momentum transfers. The orbital angular momentum transfers associated with the excitation of the 3022- and 3865-keV states cannot be established. The position in the energy spectrum and the angular distribution of the latter suggest an $l=4$ transition. The 3022-keV level may be the same state as the 3014-keV level observed in the (d, p) reaction (see Table IV).

IV. COMPARISON WITH CALCULATIONS

In the simplest shell-model description of ^{206}Tl, the (t, α) reaction would only excite five doublets, as discussed in the Introduction. Because many additional states have been observed, it is necessary in a description of the level scheme to include the effects of residual interactions between the neutron hole and the proton hole. Kuo[22] has calculated the excitation spectrum of ^{206}Tl using a realistic (Hamada-Johnson) nucleon-nucleon interaction. He considers states of spin 0–8 up to 7.5-MeV excitation. All one- and two-oscillator excitations of the ^{208}Pb core are included. Kuo finds rather large configuration mixing; in particular, the $d_{3/2}^{-1}$ and $d_{5/2}^{-1}$ mixtures are often quite large. Indeed, the experimental results on the $(p_{1/2}^{-1})_\nu(d_{3/2}^{-1})_\pi$ doublet (see Table III) suggest that the combined strength is considerably less than the $d_{3/2}$ strength in ^{207}Tl, and similarly for the $(d_{5/2}^{-1})_\pi$ strength. Also, the majority of the extra levels observed are populated by $l=2$ orbital transfers. In contrast, 80–90% of the strength of the $(3s_{1/2}^{-1})_\pi$ and $(1h_{11/2}^{-1})_\pi$ proton-hole states is found in the corresponding doublets.

For each calculated two-hole wave function of spin J, there are at most two components which can be formed by the ^{207}Pb$(t, \alpha)^{206}$Tl reaction. They are $(3p_{1/2}^{-1})_\nu(n_1l_1j_1^{-1})_\pi$ and $(3p_{1/2}^{-1})_\nu(n_2l_2j_2^{-1})_\pi$, with amplitudes a_{j1} and a_{j2}, where j_1 or $j_2=J\pm\frac{1}{2}$. The predicted cross section for exciting this state, based on the observed cross sections to one hole states in ^{207}Tl is

$$\sigma_{\mathrm{Kuo}}{}^J=\sigma_{\mathrm{STAT}}{}^J(j_1)a_{j_1}{}^2+\sigma_{\mathrm{STAT}}{}^J(j_2)a_{j_2}{}^2.$$

Figures 15 and 16 compare the observed positions and intensities of levels populated by momentum transfer l, to the positions and intensities predicted by the calculations of Kuo[22] using the above expression. Lines connect those states that are believed to correspond.

Inspection of the calculated wave functions shows that only for very weakly excited levels does more than one component contribute. Insofar as this is actually true for the real wave function of the states, one can check the sum rule

$$\sum\sigma_{\max}{}^J=\sigma_{\mathrm{STAT}}{}^J(j),$$

where the sum is over all states of spin J observed with momentum transfer j. These are compared in Table V using the identifications suggested by Figs. 15 and 16.

Kuo's calculations reproduce many features of the experimental spectrum. The predicted strengths of the doublets given in column 6 of Table III are within 20% of the experimental strengths. The set of all $l=2$ transitions is shown in Fig. 15. The positions and intensities of the levels at 273, 647, 1002, 1653, 1852, and 2061 keV are qualitatively in agreement. The 635- and 806-keV states are also predicted. A group of states near 1.5 MeV in the theoretical spectrum should appear as poorly resolved states with a large over-all cross section and is not found. The state observed in the (n, γ), (d, p) and (t, α) experiments at about 1120 keV could belong to this group.

The $l=0$ transfer spectrum [Fig. 16(a)] contains states with a $(3p_{1/2}^{-1})_\nu(3s_{1/2}^{-1})_\pi$ configuration as a

TABLE V. Test of the sum rule for each l_π and J.

l_π	J^π	$\sum\sigma_{\max}{}^J(^{206}\mathrm{Tl})$ (mb)	$\sigma_{\mathrm{STAT}}{}^J(j)$ (mb)
$l=0$	0^-	0.16	0.24
	1^-	0.60	0.71
$l=2$	1^-	0.52	0.46
	2^-	0.93(1.34)	1.39
	3^-	0.70	0.87
$l=5$	5^+	0.53	0.46
	6^+	0.60	0.54

component. The low-lying doublet is reproduced in intensity and position. The states near 1.3 MeV, however, are not seen in the experimental spectrum. The $l=5$ transfer spectrum [Fig. 16(b)] contains states with a $(3p_{1/2}^{-1})_\nu(1h_{11/2}^{-1})_\pi$ configuration as a component. The calculations reproduce the experimental spectrum rather well.

Use of the above sum rule and the level assignments suggested by Figs. 15 and 16 gives good agreement with the expected total strength (see Table V). Column 3 of Table V is the summed cross sections from Table IV. Column 5 is the expected total strength taken from Table III and based on the ^{208}Pb(t, α)^{207}Tl cross sections. Notice that the 2^- states can be formed both by $2d_{3/2}$ and $2d_{5/2}$ transfers. The assigned 2^- states make up 70% of the sum rule. If all unassigned $l=2$ transitions are treated as $J^\pi=2^-$ states, then the summed cross section is 1.34 mb as indicated in the parentheses. This exhausts the sum rule. In general, there is very good quantitative agreement, indicating that the suggested correspondence between observed and calculated levels is self-consistent.

V. CONCLUSIONS

The present study has shown that in the ^{208}Pb(t,α)^{207}Tl reaction, the three lowest-lying states of ^{207}Tl yield relative spectroscopic factors which are consistent with the expected strengths based on the shell model. It is also concluded that the two remaining strong states in the spectrum ($d_{5/2}^{-1}$ and $g_{7/2}^{-1}$) may contain only 60 and 40% of the expected single-particle strength, respectively, relative to the first three. We have also found additional levels, not observed previously, above 3500-keV excitation.

In the reaction ^{207}Pb(t, α)^{206}Tl, the most strongly populated levels in the spectrum are the members of four doublets which arise from the coupling of a $3p_{1/2}$ neutron hole to proton holes. The experimental spectrum observed in the ^{207}Pb(t, α)^{206}Tl reaction has been compared with a theoretical calculation of the proton-hole–neutron-hole states of ^{206}Tl,[22] and we find that the calculations show many of the features of the experimental data. Indeed, the impressive quantitative agreement for the strongly excited states (Table III) is encouraging support for Kuo's description of the neutron-hole–proton-hole interaction in the ^{208}Pb region. Finally, the identification of observed states with calculated states (Figs. 15 and 16) makes possible a sum-rule check of the total strength observed in ^{206}Tl with the strength observed in ^{207}Tl. They are in quantitative agreement (Table V).

ACKNOWLEDGMENTS

We gratefully acknowledge the excellent scanning of the Los Alamos Scientific Laboratory scanning group, the assistance of the operators at the tandem accelerator, and we thank Mrs. Judith C. Gursky for fabricating the target.